BioSystems 103 (2011) 212–223

Contents lists available at ScienceDirect

BioSystems

journal homepage: www.elsevier.com/locate/biosystems

Spatiotemporal dynamics of the Calvin cycle: Multistationarity and symmetry breaking instabilities

Sergio Grimbs[a], Anne Arnold[a,b], Aneta Koseska[c], Jürgen Kurths[d,e], Joachim Selbig[a,b], Zoran Nikoloski[a,b,*]

[a] Institute of Biochemistry and Biology, University of Potsdam, Germany
[b] Max-Planck Institute of Molecular Plant Physiology, Germany
[c] Interdisciplinary Center for Dynamics of Complex Systems, University of Potsdam, D-14476 Potsdam, Germany
[d] Potsdam Institute for Climate Impact Research, D-14412 Potsdam, Germany
[e] Institute of Physics, Humboldt University Berlin, D-10099 Berlin, Germany

ARTICLE INFO

Article history:
Received 1 July 2010
Received in revised form 18 October 2010
Accepted 26 October 2010

Keywords:
Multistationarity
Calvin cycle
Algebraic geometry
Bifurcation parameters
Biomass

ABSTRACT

The possibility of controlling the Calvin cycle has paramount implications for increasing the production of biomass. Multistationarity, as a dynamical feature of systems, is the first obvious candidate whose control could find biotechnological applications. Here we set out to resolve the debate on the multistationarity of the Calvin cycle. Unlike the existing simulation-based studies, our approach is based on a sound mathematical framework, chemical reaction network theory and algebraic geometry, which results in provable results for the investigated model of the Calvin cycle in which we embed a hierarchy of realistic kinetic laws. Our theoretical findings demonstrate that there is a possibility for multistationarity resulting from two sources, homogeneous and inhomogeneous instabilities, which partially settle the debate on multistability of the Calvin cycle. In addition, our tractable analytical treatment of the bifurcation parameters can be employed in the design of validation experiments.

1. Introduction

The development of techniques for increasing plant biomass holds the promise of engineering plants which can be used for production of biofuels in a sustainable carbon-neutral fashion. Plant biomass is the outcome of complex biochemical reactions reflecting the necessity for balancing conflicting demands for resources to maintain cell vitality and function with those to support growth. Plant growth depends on the uptake and assimilation of inorganic nutrients and the photosynthetic assimilation of carbon dioxide (CO_2) via the Calvin cycle (Stitt and Krapp, 1999). This CO_2-assimilating pathway takes place in the chloroplast of photosynthetic plant cells yielding carbon skeletons necessary for maintenance of the entire plant metabolism. Therefore, understanding the mechanisms of the Calvin cycle can propel the design of techniques for manipulation of its efficiency.

The study of cell metabolism has traditionally focused on determining the factors that influence metabolic rates, at levels of both metabolic pathways and the whole organism (Heinrich and Schuster, 1996). Although there has been a significant progress in the structural analysis of metabolic pathways in order to understand and predict the distribution of cellular fluxes (Palsson, 2000; Schuster et al., 2000; Grimbs et al., 2007), addressing the problem of efficient biomass production requires elucidation of the dynamical properties of plant metabolic models. The question arises as to whether there exists a qualitative dynamical feature of plant-specific metabolic pathways which results in possibilities for increasing the production of biomass.

Multistationarity is a qualitative feature of systems, characterized by the existence of multiple positive steady states, with great potential for application in biotechnology. Biological entities (*i.e.*, genes, proteins), biochemical pathways, and cells operate in one of multiple exclusive states at any given time. For instance, a gene can either be expressed or not expressed, glycolysis and gluconeogenesis represent mutually exclusive metabolic states, and a stem cell may be at an undifferentiated state or committed to differentiating to a particular lineage (Chatterjee et al., 2008). As pointed out in Prigogine and Nicolis (1967), there are at least two sources for multistationarity: (1) instabilities with respect to space-independent (*homogeneous*) perturbations, whereby the system goes from one to another homogeneous steady state, which may or may not be stable, and (2) instabilities with respect to space-dependent (*inhomogeneous*) perturbations, when the diffusion plays a crucial role by increasing the manifold of possible perturbations. From a biotechnological perspective, altering the control of multistationarity in

* Corresponding author at: Max-Planck Institute of Molecular Plant Physiology, Am Muehlenberg 1, 14476 Potsdam, Germany. Tel.: +49 331 567 8630.
E-mail address: nikoloski@mpimp-golm.mpg.de (Z. Nikoloski).

0303-2647/$ – see front matter © 2010 Elsevier Ireland Ltd. All rights reserved.
doi:10.1016/j.biosystems.2010.10.015

biological systems offers means for manipulating the outcome of a particular biochemical process.

Given a stimulus, the control of a biological switch, characterized with two *stable* steady states, is established via perturbation of the stimulus' concentration: When it changes over a threshold value, the entire system undergoes a transition from one to the other stable state, without residing in an in-between state due to the instability of the latter. The stimulus which exhibits such a property is referred to as *bifurcation parameter*. Bifurcation parameters can be endogenous or exogenous to the system. Typical endogenous bifurcation parameters include the kinetic parameters associated with a particular biochemical reaction, while exogenous parameters include conservation relations of some chemical element. We note that the response of individual biochemical reactions to changes in the bifurcation parameter is continuous and graded; however, the combination of these graded responses gives rise to a bistable (switching) behavior.

For experimental validation of bistability, one relies on the threshold property for the applied stimulus: The threshold concentrations of the stimulus for the two possible transitions between the steady states (from the first to the second steady state and vice versa) are different. Therefore, two response curves can be generated by adding/subtracting small increments of the stimulus, resulting in a *hysteresis diagram*. However, such experimental approaches on a population level could have contradicting results; namely, the compounded effect of the individual bistable cellular responses may appear graded for the population itself. The contrast between population and single cell levels has been illustrated experimentally in a number of systems, including *Xenopus levis* oocytes (Bagowski et al., 2001, 2003). We point out that the experimental set up for monitoring the photosynthetic response in plants may be further hindered by the heterogeneous population of cells in a leaf or a rosette, since not all cells demonstrate photosynthetic capacity. However, experimental approaches relying on isolated chloroplasts may prove useful in the study of the existence of multistationarity in photosynthetic processes.

The theoretical analysis of multistationarity in biological systems is performed on a kinetic model comprising a set of biochemical reactions. Therefore, any conclusions regarding multistationarity of the studied system ultimately depend on the employed model. The general numerical approach relies on conducting stability analysis of a given model through the following steps: (1) a steady state is calculated, (2) perturbation of the system is imposed to establish the stability of the steady state, (3) perturbation of the stimulus' concentration is imposed to check the transition to a new (stable) steady state. The existing studies focus on multistationarity (and multistability) in gene-regulatory and signaling networks (Kaneko and Yomo, 1994; Nakajima and Kaneko, 2008; Koseska et al., 2010; Tyson et al., 2003).

Unlike gene-regulatory and signaling networks, metabolic pathways with capacity for multistationarity can be characterized intuitively as transiting between states which result in different composition and quantity of biomass. Development of detailed kinetic models of metabolic pathways, however, requires information about the rate equations, enzyme-specific kinetic parameters, and substrate/product regulatory mechanism. Nevertheless, recently established mathematical approaches render it possible to infer sound statements about multistationarity of metabolic networks even when kinetic parameters are not known.

With respect to the multistationarity of a set of biochemical reactions, two questions are crucial: (1) Do the biochemical reactions have the capacity for multistationarity irrespective of the kinetic parameters? and (2) Given a (partial) set of kinetic parameters, which element of the biochemical reactions can be considered a bifurcation parameter? To answer the first question, one needs to establish a relation between multistationarity and the underlying structure of the biochemical reactions. Knowing whether a network can operate in more than one steady state only partially addresses the multistationarity analysis, since one still has to determine the regions of the parameter space in which multistationarity occurs. The answer to the second question pinpoints precisely these regions.

Due to the potential for biotechnological applications of multistationarity, the question as to whether the Calvin cycle could operate in multiple steady states is of paramount importance. Despite the large number of models for the Calvin cycle, the analysis of the existence and experimental validation of multiple steady states in this pathway is still fragmentary, usually resulting in contradictory conclusions. Pettersson and Ryde-Pettersson (1988) found two steady states for their model of the Calvin cycle. However, they showed that one of these steady states is unstable and therefore considered to be of no biological relevance, while the remaining stable steady state was in accordance with previous experiments (Flügge et al., 1980; Heldt et al., 1977). Poolman et al. (2000) also demonstrated that their extension of the model of Pettersson and Ryde-Pettersson (1988) exhibits two steady states. Moreover, Poolman et al. (2001) attempted to experimentally verify this result; however, the two observed steady states were found in leafs of different age and therefore have different capacities of utilizing the produced carbohydrates (Olçer et al., 2001). It is still unclear to which extent these results hold within one single chloroplast or leaf. A systematic approach was taken by Zhu et al. (2009), using a sophisticated algorithm to find all roots of a system of polynomials. The application of this approach to a simple model of the Calvin cycle revealed 40 steady states, of which 39 were biological infeasible due to extremely small or even negative metabolite concentrations. Although this analysis was limited to a given set of kinetic parameters, Zhu et al. (2009) concluded that the Calvin cycle can operate in only one steady state.

Here we systematically analyze the capacity for multiple steady states in a model of the Calvin cycle endowed with a hierarchy of kinetic laws based on two mathematical approaches: Chemical Reaction Network Theory (CRNT), together with its extension based on elementary flux modes, and algebraic geometry. The hierarchy of kinetic laws imposed on the set of biochemical reactions describing the Calvin cycle offers the means for determining the necessary and sufficient conditions for the existence of two steady states in this particular model. Moreover, we determine the set of bifurcation parameters which could be helpful in experiment design for validation of our theoretical findings. In addition, we explore the possibility for the existence of symmetry breaking instabilities in a slightly modified model of the Calvin cycle. Our results partially settle the debate about the existence of multistability in a model of the Calvin cycle and contribute an alternative interpretation of the existing experimental data.

The paper is organized as follows: In Section 2 we briefly review the mathematical apparatus needed for studying the relation between the structure of the Calvin cycle and its capacity for multistationarity. The hierarchy of kinetic laws embedded in the Calvin cycle is described in Section 3. The general approach is outlined in Section 4 and then applied in Section 5. We present our findings for the existence of multiple steady states in a model of the Calvin cycle for four types of kinetics: mass action, Michaelis–Menten via mass action, irreversible Michaelis–Menten, and mass action with diffusion kinetics, in Sections 5.1–5.4, respectively. Finally, in Section 6, we conclude with the implications or our findings and the necessity of a carefully tailored experiment for validation.

2. The Structure of a Model for the Calvin Cycle

The Calvin cycle consists of three phases in which there is energy supply in form of ATP and redox elements (NADP/NADPH):

Table 1
Biochemical reactions in a simple model of the Calvin cycle. First column gives the rate constants for the seven irreversible reactions. The biochemical reactions and their simplifications, due to model assumptions, appear in the second and third column of the table, respectively. The names of the enzymes catalyzing these reactions are given in the last column.

Rate const.	Reactions		Enzyme name
	Biochemical	Simplified	
k_1	RuBP + CO_2 → 2PGA	RuBP → 2PGA	RuBisCO
k_2	PGA + ATP → ADP + DPGA	PGA → DPGA	PGA kinase
k_3	DPGA + NADPH → GAP + P + NADP	DPGA → GAP	GAP dehydrogenase
k_4	5GAP → 3Ru5P	5GAP → 3Ru5P	
k_5	Ru5P + ATP → RuBP + ADP	Ru5P → RuBP	Ru5P kinase
k_6	PGA → Sink	PGA → 0	Sink capacity
k_7	GAP → Sink	GAP → 0	Sink capacity

(1) *carboxylation*, during which the enzyme RuBisCO adds CO_2 to ribulose-1,5-bisphosphate (RuBP) to get two molecules of phosphoglycerate (PGA), (2) *reduction*, converting the obtained PGA into 1,3-diphosphoglycerate (DPGA) and glyceraldehyde-3-phosphate (GAP), and (3) *regeneration*, which recovers RuBP after several intermediate steps from ribulose-5-phosphate (Ru5P) (Berg et al., 2002). The enzymatic reactions comprising the simple model of the Calvin cycle are given by Zhu et al. (2009) and appear in the second column of Table 1. We modified the reaction of the regeneration phase from the model of Zhu et al. (2009), so that its stoichiometric coefficients are integers. Although very unlikely to occur in reality, this reaction has been included in standard textbook models of the Calvin cycle. We assume that there is a constant supply of ATP, NADPH, orthophosphate (P), and CO_2. Therefore, by assuming constancy of ATP to ADP and NADPH to NADP ratios, the equations can be rewritten as in the third column of Table 1, pictorially shown in Fig. 1.

The *reaction network*, *G*, for a given set of biochemical reactions is composed of three sets: (1) *S* is a set of *species* given by the chemical compounds occurring in the biochemical reactions, (2) *C* includes all *complexes*, where each complex is given by the left and right side of a reaction, and (3) *R* consists of *reactions*, indicating the transformation of the complexes. Therefore, *G* can be described by the 3-tuple (*S*, *C*, *R*). For the Calvin cycle model, under the simplifying assumptions, the reaction network, *H*, is fully described by

$$S(H) = \{\text{RuBP,PGA,DPGA,GAP,Ru5P}\},$$

$$C(H) = \{\text{RuBP,2PGA,Ru5P,PGA,DPGA,GAP,5GAP,0, 3Ru5P}\},$$

where 0 is the special zero complex (denoting the sink), and the set $R(H)$ is given by the third column of Table 1. The number of species, complexes, and reactions will be denoted by m, n, and r, respectively. For this reaction network, $m = 5$, $n = 9$, and $r = 7$.

Each species is associated with a continuous variable representing the species' concentration. We will use x_s, $s \in S$, to denote these variables which take only non-negative values due to physiological constraints. For the Calvin cycle network, *H*, the variables are then x_{RuBP}, x_{PGA}, x_{DPGA}, x_{GAP}, and x_{Ru5P}. Let a complex $c \in C$ be denoted by y_c. The complex y_c can be associated a vector over the set of species *S*, whose entries are given by the stoichiometric coefficients with which the species $s \in S$ participate in y_c. For instance, the complex 2PGA in $C(H)$ is described by the vector $y_{\text{2PGA}} = (0, 2, 0, 0, 0)$, and the vector representation for the zero complex 0 is the null vector $\mathbf{0}$ over the five species in $S(H)$. A reaction converting a complex c into complex c' will be denoted by $y_c \to y_{c'}$, and is associated a vector $y_{c'} - y_c$. To illustrate, the reaction $y_{\text{RuBP}} \to y_{\text{2PGA}}$ is represented by the vector $(-1, 2, 0, 0, 0)$.

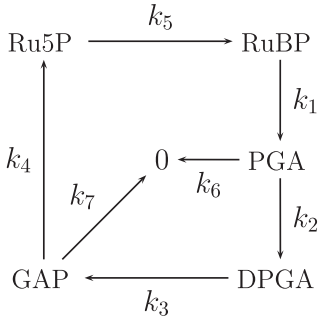

Fig. 1. Model of the Calvin cycle. The model includes seven biochemical reactions, shown in Table 1, on which different types of kinetic laws are imposed, as described in Section 3.

The vector representations of complexes can be gathered into a complex matrix *Y*, with dimensions $(m \times n)$, while the reaction vectors yield the stoichiometric matrix *N*, with dimensions $(m \times r)$. In addition, each reaction can be represented by a vector where the substrate complex takes a value of -1 and the product complex has a value of 1. Such a representation of reactions gives rise to a matrix I_a of dimensions $(n \times r)$. Upon closer observation, one may establish the trivial relation, $N = YI_a$. For the network of the Calvin cycle model, the matrices *N* and I_a are given by:

$$N(H) = \begin{bmatrix} -1 & 0 & 0 & 0 & 1 & 0 & 0 \\ 2 & -1 & 0 & 0 & 0 & -1 & 0 \\ 0 & 1 & -1 & 0 & 0 & 0 & 0 \\ 0 & 0 & 1 & -5 & 0 & 0 & -1 \\ 0 & 0 & 0 & 3 & -1 & 0 & 0 \end{bmatrix}, \tag{1}$$

and

$$I_a(H) = \begin{bmatrix} -1 & 0 & 0 & 0 & 1 & 0 & 0 \\ 1 & 0 & 0 & 0 & 0 & 0 & 0 \\ 0 & 0 & 0 & 0 & -1 & 0 & 0 \\ 0 & -1 & 0 & 0 & 0 & -1 & 0 \\ 0 & 1 & -1 & 0 & 0 & 0 & 0 \\ 0 & 0 & 1 & 0 & 0 & 0 & -1 \\ 0 & 0 & 0 & -1 & 0 & 0 & 0 \\ 0 & 0 & 0 & 0 & 0 & 1 & 1 \\ 0 & 0 & 0 & 1 & 0 & 0 & 0 \end{bmatrix}. \tag{2}$$

We will denote the rank of the stoichiometric matrix *N* by *q*. For a stoichiometric matrix with *m* rows, there then exist $m - q$ conservation relationships. Each conservation relationship gives rise to a stoichiometric compatibility class that have important consequences for the study of steady states; namely, the multistationarity corresponds to the existence of more than one steady state in *one* stoichiometric compatibility class.

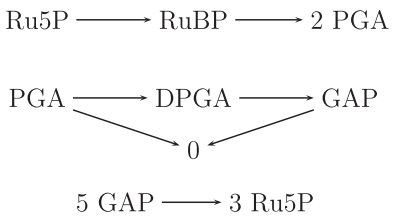

Fig. 2. Reaction network for the model in Fig. 1 with mass action kinetics. There are three linkage classes, given by the connected components {Ru5P, RuBP, 2PGA}, {PGA, DPGA, GAP, 0}, and {5GAP, 3RuBP}.

Note that the matrix I_a can be associated a directed graph representation, in which the nodes are the complexes of the reaction network and the directed edges are given by the entries of I_a, considered as an incidence matrix. The resulting graph may have one or more connected components, which are termed *linkage classes* (Feinberg, 1995a). The number of linkage classes is denoted by l. For the model in Fig. 1, under the assumption of mass action kinetics, the reaction network has three linkage classes, $l = 3$, depicted in Fig. 2. Each linkage class can further be decomposed into *strong linkage classes*. A strong linkage class is the maximal strongly connected subgraph of the directed graph associated to a reaction network (in a strongly connected subgraph, there is a directed path from a node u to v and vice versa) (Feinberg, 1995a). If no edge from a complex inside a strong linkage class to a complex outside exists, we have a *terminal strong linkage class*.

Next, we define the deficiency of a reaction network, based on which one can draw conclusions about the existence of bistability. The *deficiency* of a reaction network G, $\delta(G)$ is defined as $\delta(G) = m - l - q$, and can, therefore, be calculated directly from the structure of the reaction network (Feinberg, 1995a). Note that the deficiency of a linkage class is calculated in the same way as for the entire reaction network. The following two theorems establish the needed relation between the dynamics and structure of a reaction network (Feinberg, 1995a):

Theorem 2.1. (Deficiency Zero Theorem) *If the deficiency of a reaction network is zero, then, assuming mass-action kinetics for all reactions, no set of positive parameter values for k exists that leads to multiple steady states.*

Theorem 2.2. (Deficiency One Theorem) *Given a reaction network, if the following conditions are satisfied*:

(1) *The deficiency of each linkage class is less or equal to one*,
(2) *The deficiencies of all linkage classes sum up to the deficiency of the entire network, and*
(3) *Each linkage class contains precisely one terminal strong linkage class*,

then no positive parameter values for k exist that allow multistationarity.

Note that Theorem 2.2 extends the result of Theorem 2.1 and applies to a larger ensemble of networks. These theorems can be used to establish if a given network *does not* have the capacity for multiple steady states. If the network is of deficiency one, the Deficiency One Algorithm (D1A) can be used to determine the two steady states for the analyzed network. The Deficiency One Algorithm has been implemented in the *chemical reaction network toolbox* (Feinberg and Ellison, 2000). However, the current version is restricted to reaction networks of at most 20 complexes due to computational limitations, which is already too small for most biochemical networks. Recently, the MATLAB package ERNEST was introduced by Soranzo and Altafini (2009) to overcome this restriction for a subset of reaction networks.

Conradi et al. (2007) have addressed the problem of resolving multistationarity of large networks by analyzing special subnetworks. In particular, they investigated subnetworks defined by elementary flux modes called *stoichiometric generators*. An elementary flux mode of a reaction network is a minimal set of reactions which can operate at steady state (Schuster et al., 2000). An elementary flux mode E is a stoichiometric generator if $I_c E \neq 0$. Conradi et al. (2007) have shown that stoichiometric generators are of deficiency one, so they are amenable for an analysis based on the D1A. If the subnetwork implied by a stoichiometric generator is capable of supporting two steady states, then these steady states might be extended to the initial network. The authors provide additional conditions under which the bistability of the subnetwork can be extended on the entire network. However, if no multistability is found for any of the subnetworks, the multistationarity of the entire network remains unresolved. Altogether, this approach allows for analyzing reaction networks of previously intractable sizes by decomposing them into smaller subnetworks. It is worth pointing out that the calculation of all elementary flux modes can be computational demanding (Klamt and Stelling, 2002; Acuña et al., 2008).

3. Hierarchy of Kinetic Laws

To establish the relationship between the structure of a reaction network G and the system of differential equations capturing the dynamics, one needs to consider the type of the employed kinetics. The kinetics for a reaction network $G = (S, C, R)$ involves a function that describes the rate at which the chemical species interact as substrates and are transformed into products. Here, we briefly review the types of kinetics which are considered in the rest of the analysis: mass action (MA), Michaelis–Menten represented in terms of mass action (MM-MA), and the classical irreversible Michaelis–Menten (MM).

In mass action kinetics, the rate of a reaction is proportional to the concentration of the reactant multiplied by a kinetic constant. In general, a substrate s, with concentration x_s, which participates with y_s molecules in the substrate complex of a reaction, contributes $x_s^{y_s}$ to the rate of the reaction. Therefore, the mass action kinetics of the reaction $y_c \to y_{c'}$ can be written as:

$$v_{y_c \to y_{c'}}(k, x) = k_{y_c \to y_{c'}} \prod_{s \in S \cap supp(y_c)} x_s^{y_s}, \tag{3}$$

where $supp(y_c) = \{s \mid y_c(s) \neq 0\}$.

Since Michaelis–Menten kinetics of a reaction $A \to B$ catalyzed by enzyme E can be derived from three mass action reactions $A + E \to AE$, $AE \to A + E$, and $AE \to B$, here we use Michaelis–Menten kinetics represented in terms of mass action. Applying this kinetic requires that each irreversible reaction is substituted by three reactions with mass action kinetics.

In irreversible MM kinetics with more than one substrate, the rate of a reaction $A + B \to C + D$ can be written as:

$$v(k, x) = V_m \frac{x_A x_B}{(x_A + K_{mA})(x_B + K_{mB})}, \tag{4}$$

where K_{mA} and K_{mB} are the MM constants for the substrates A and B, and V_m is the maximum rate of the reaction.

The model of the reaction network G together with a specified kinetics $v(k, x)$ is succinctly written as:

$$\frac{dx}{dt} = N \cdot v(k, x). \tag{5}$$

Note that the right-hand side of Eq. (5) defines a set of rational functions expressed as ratios of two polynomials. Assuming diffusion of one system element, Eq. (5) can also be rewritten for

the reaction diffusion system in one dimension in a form involving partial derivatives for any of the three kinetic laws discussed above.

4. General Approach

In this section, we describe our general method for determining the existence of multistationarity in a model specified by Eq. (5). Given a reaction network G together with parameter-dependent reaction rates $v(k, x)$ first we check if Theorems 2.1 and 2.2 from CRNT (Horn and Jackson, 1972; Feinberg, 1995a,b) are applicable on the entire network. If this is not the case, we employ subnetwork analysis described in Section 2. To determine the bifurcation parameters, we rely on finding a *rational parameterization* for the system of polynomials given in Eq. (5), whereby a small subset of variables can be identified in terms of which all others can be calculated at steady state (Thomson and Gunawardena, 2009). For further reading on the concept of Gröbner basis, the interested reader is directed to Cox et al. (1991). The steps of our analysis are summarized in Algorithm 1.

Our approach is partly based on algebraic geometry, described in Gatermann and Wolfrum (2005). Similar approaches have recently been introduced for the analysis of multistationarity in protein phosphorylation and apoptosis (Martinez-Forero et al., 2010; Thomson and Gunawardena, 2009; Li and Ho, 2000). Although the steps outlined in Algorithm 1 can be used to determine the existence of multistationarity together with the bifurcation regions, additional steps must be taken to establish the stability of the determined steady states. The details of the methods from algebraic geometry are illustrated in the Result's section pertaining to Michaelis–Menten kinetics, which renders the presentation of the results easier to follow.

Algorithm 1. Steps in multistationarity analysis

Data: G reaction network,
N stoichiometric matrix,
$v(k, x)$ reaction rates
Result: Answer to multistationarity,
Set of bifurcation parameters
begin
  Determine deficiency, δ, of G
  if $v(k, x)$ *is MA or MM-MA* **then**
    if *($\delta = 0$) $\wedge$ (Theorem 2.1 holds)* **then**
      No multistationarity for any choice of k
    else if $\delta > 1$ **then**
      if *Theorem 2.2 holds* **then**
        No multistationarity for any choice of k
      else if *D1A is applicable* **then**
        Multistationarity for k as outcome of D1A
      else
        Determine stoichimetric generators
        Apply the approach of Conradi et al. (2007)
  else
    Reduce N to its reduced echelon form N_{re}
    Identify stoichiometric compatibility classes M (conservation relations $m - q$)
    Construct a system of polynomials, V, from $N_{re} \cdot v(k, x)$ and adding M
    Calculate the Gröbner bases of V (*e.g.*, by using lexicographic order)
    Determine bifurcation parameters β by solving $p = 0$, $p \quad V$, in terms of β

5. Results

Here we describe the results of applying Algorithm 1 to the model of the Calvin cycle in which the hierarchy of kinetics, described in Section 3, is embedded.

5.1. Mass Action Kinetics

The model in Fig. 1 with mass action kinetics results in a reaction network depicted in Fig. 2. It is of deficiency one and composed of three linkage classes, each of deficiency zero; therefore, neither Theorem 2.1 nor Theorem 2.2 is applicable. However, by applying D1A, we conclude that no multiple positive steady states are possible, no matter what values of the mass-action kinetic parameters k_i, $1 \le i \le 7$, are chosen.

Moreover, we point out that even the existence of a single steady state is not ensured and depends on some of the kinetic parameters. This conclusion can be obtained by analyzing the following system of differential equations associated with the reaction network:

$$\begin{aligned}
\frac{dx_{\mathrm{RuBP}}}{dt} &= k_5 \cdot x_{\mathrm{Ru5P}} - k_1 \cdot x_{\mathrm{RuBP}} \\
\frac{dx_{\mathrm{PGA}}}{dt} &= 2 \cdot k_1 \cdot x_{\mathrm{RuBP}} - k_2 \cdot x_{\mathrm{PGA}} - k_6 \cdot x_{\mathrm{PGA}} \\
\frac{dx_{\mathrm{DPGA}}}{dt} &= k_2 \cdot x_{\mathrm{PGA}} - k_3 \cdot x_{\mathrm{DPGA}} \\
\frac{dx_{\mathrm{GAP}}}{dt} &= k_3 \cdot x_{\mathrm{DPGA}} - 5 \cdot k_4 \cdot x_{\mathrm{GAP}}^5 - k_7 \cdot x_{\mathrm{GAP}} \\
\frac{dx_{\mathrm{Ru5P}}}{dt} &= -k_5 \cdot x_{\mathrm{Ru5P}} + 3 \cdot k_4 \cdot x_{\mathrm{GAP}}^5
\end{aligned} \tag{6}$$

To obtain the steady state solutions, the left-hand sides of Eqs. (6) are set to zero. Expressing every variable in terms of x_{RuBP} leads to $x_{\mathrm{Ru5P}} = (k_1/k_5) \cdot x_{\mathrm{RuBP}}$ and $x_{\mathrm{PGA}} = 2 \cdot k_1/(k_2 + k_6) \cdot x_{\mathrm{RuBP}}$. Subsequent

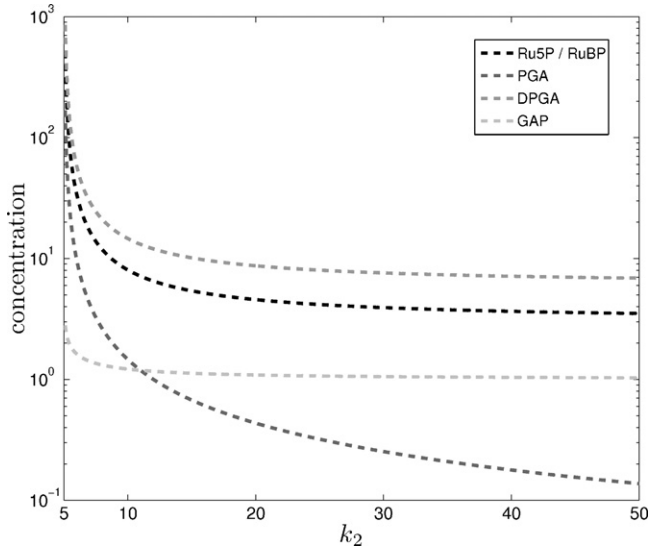

Fig. 3. Steady state concentrations for the reaction network in Fig. 2. The parameter k_2 is varied and all other parameters are fixed to 1. As k_2 approaches $5 \cdot k_6$, the concentrations go to infinity. For even smaller values of k_2, no steady state exists at all. All steady states are unstable, as indicated by the dotted lines. The concentrations x_{Ru5P} and x_{RuBP} are always the same.

substitutions yield $x_{\mathrm{DPGA}} = (k_2/k_3) \cdot x_{\mathrm{PGA}} = 2 \cdot k_1 \cdot {}_3/k_3 \cdot (k_2 + k_6) \cdot x_{\mathrm{RuBP}}$ and $x_{\mathrm{GAP}} = \sqrt[5]{k_1 \cdot /3 \cdot k_4 \cdot x_{\mathrm{RuBP}}}$. Finally, one may obtain:

$$\begin{aligned} 0 &= k_3 \cdot x_{\mathrm{DPGA}} - k_7 \cdot x_{\mathrm{GAP}} - 5 \cdot k_4 \cdot x_{\mathrm{GAP}}^5 \\ &= \frac{2 \cdot k_1 \cdot k_2}{(k_2 + k_6)} - k_7 \cdot \sqrt[5]{\frac{k_1}{3 \cdot k_4} \cdot x_{\mathrm{RuBP}}} - \frac{5}{3} \cdot k_1 \cdot x_{\mathrm{RuBP}} \\ &= \left(\frac{2 \cdot k_1 \cdot k_2}{(k_2 + k_6)} - k_7 \cdot \sqrt[5]{\frac{k_1}{3 \cdot k_4 \cdot x_{\mathrm{RuBP}}^4}} - \frac{5}{3} \cdot k_1 \right) \cdot x_{\mathrm{RuBP}} \end{aligned} \tag{7}$$

Note that Eq. (7) has five distinct solutions, of which only one is a positive real number, given by:

$$x_{\mathrm{RuBP}} = \sqrt[4]{\frac{k_1 \cdot k_7^5}{3 \cdot k_4 \left(\frac{2 \cdot k_1 \cdot k_2}{k_2 + k_6} - \frac{5}{3} \cdot k_1 \right)^5}}$$

for $(2 \cdot k_1 \cdot k_2/(k_2 + k_6)) - 5/3 \cdot k_1 > 0$ or equivalently $k_2 > 5 \cdot k_6$. This imposes a lower bound for k_2 in terms of k_6. More precisely, if k_2 is below this bound, not even a single steady state exists, no matter what values are obtained for all remaining parameters k. The change of steady state concentration for varying k_2, while keeping all other k's fixed to one, is shown in Fig. 3.

To analyze the stability of the determined steady state, one has to calculate the eigenvalues of the Jacobian matrix, J, of the system given in Eqs. (6). The Jacobian is given by:

$$J = \begin{bmatrix} k_5 & -k_1 & 0 & 0 & 0 \\ 0 & 2 \cdot k_1 & -k_2 - k_6 & 0 & 0 \\ 0 & 0 & k_2 & -k_3 & 0 \\ 0 & 0 & 0 & k_3 & -25 \cdot k_4 \cdot x_{\mathrm{GAP}}^4 - k_7 \\ -k_5 & 0 & 0 & 0 & 15 \cdot k_4 \cdot x_{\mathrm{GAP}}^4 \end{bmatrix}. \tag{8}$$

The roots of the characteristic polynomial $\chi_J(\lambda) = \det(J - \lambda \cdot I)$, where I stands for the identity matrix, determine the eigenvalues of J. The characteristic polynomial can be calculated by a subsequent minor expansion across the first row of Eq. (8), leading to:

$$\begin{aligned} \chi_J(\lambda) = (k_5 - \lambda)(k_1 + \lambda)(k_2 + k_6 + \lambda)(k_3 + \lambda)(25k_4 x_{\mathrm{GAP}}^4 + k_7 \\ + 30k_5 k_1 k_2 k_3 k_4 x_{\mathrm{GAP}}^4). \end{aligned} \tag{9}$$

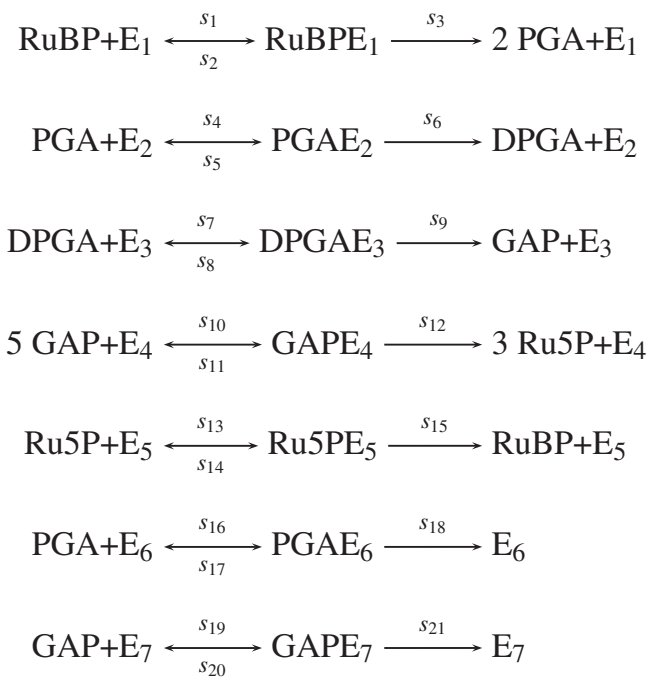

Fig. 4. Reaction network for model in Fig. 1 with Michaelis–Menten via mass action kinetics. There are seven linkage classes, given by the connected components of the graph.

The expansion of χ_J in Eq. (9) in the form $\chi_J(\lambda) = \alpha_0\lambda^0 + \alpha_1\lambda^1 + \alpha_2\lambda^2 + \alpha_3\lambda^3 + \alpha_4\lambda^4 + \alpha_5\lambda^5$ may be used to show that α_1 to α_5 are negative. The remaining coefficient α_0 can be expressed as $\alpha_0 = k_5 k_1 k_3 \left(k_7 (-k_2 - k_6) + 5k_4 x_{\mathrm{GAP}}^4 (k_2 - 5k_6) \right)$. Substituting $x_{\mathrm{GAP}}^4 = k_7/k_4(6k_2/(k_2 + k_6) - 5)$, obtained from the steady state relation between x_{RuBP} and x_{GAP}, one finally gets

$$\alpha_0 = 4k_5 k_1 k_3 k_7 (k_2 + k_6).$$

Hence, α_0 is always positive. From Descartes' rule of sign it follows that $\chi_J(\lambda)$ has exactly one positive root and therefore one positive eigenvalue. Consequently, the entire parameter space of the system, given in Eqs. (6), does not contain any stable steady states, which clearly makes this network, with mass action kinetics, an extremely poor model.

5.2. Michaelis–Menten Via Mass Action Kinetics

If the kinetics of the model in Fig. 1 is assumed to be Michaelis–Menten represented by mass action, as described in Section 3, the I_a matrix of the reaction network is depicted as in Fig. 4. This reaction network has a deficiency of 2 and is composed of seven linkage classes, each of deficiency 0. Therefore, neither Theorems 2.1 and 2.2 nor D1A are applicable. Furthermore, since the network consists of 21 complexes, it already exceeds the computational capabilities of the CRNT Toolbox (Feinberg and Ellison, 2000).

Conradi et al. (2007) proposed a method to draw conclusions about multistationarity of a reaction network by analyzing special subnetworks. In particular, they investigated subnetworks defined by elementary flux modes (Schuster et al., 2000) and elucidated under which conditions results for these subnetworks also hold for the entire network.

Applying this approach, subnetwork analysis revealed only two elementary modes, which were calculated using the Metatool pack-

Table 2
Parameter assignment for the system given in Eqs. (10) which allow for multiple positive steady states. Parameters set to 1 are precisely those associated with reactions that are not present in the first elementary mode which was used to construct a subnetwork. For simplicity, all parameters are chosen to have the same value.

s_1	=	0.99119923	s_8	=	1	s_{15}	=	2.4579323
s_2	=	1	s_9	=	6.6747969	s_{16}	=	1
s_3	=	2.0237445	s_{10}	=	15.141035	s_{17}	=	1
s_4	=	9.9649223	s_{11}	=	1	s_{18}	=	1
s_5	=	1	s_{12}	=	0.26920841	s_{19}	=	1.5770407
s_6	=	10.30969	s_{13}	=	1.3666169	s_{20}	=	1
s_7	=	6.1626543	s_{14}	=	1	s_{21}	=	1.7182818

age (van Kamp and Schuster, 2006):

$$\nu_1^{EM} = \{3, 0, 3, 6, 0, 6, 6, 0, 6, 1, 0, 1, 3, 0, 3, 0, 0, 0, 1, 0, 1\},$$
$$\nu_2^{EM} = \{3, 0, 3, 5, 0, 5, 5, 0, 5, 1, 0, 1, 3, 0, 3, 1, 0, 1, 0, 0, 0\}.$$

These elementary modes arise from shutting down one of the two transporter reactions.

Both elementary modes, ν_1^{EM} and ν_2^{EM}, are capable of supporting two steady states, which can be calculated by the CRNT Toolbox. Furthermore, by means presented by Conradi et al. (2007), these steady states of the subnetworks induced by the elementary modes can be extended to the full network. To see this, consider the following system of differential equations obtained from the reaction network in Fig. 4:

$$\begin{aligned}
\frac{d\mathrm{RuBP}}{dt} &= s_{15}\cdot \mathrm{Ru5P}E_5 - s_1\cdot \mathrm{RuBP}\cdot E_1 + s_2\cdot \mathrm{RuBP}E_1\\
\frac{dE_1}{dt} &= -s_1\cdot \mathrm{RuBP}\cdot E_1 + s_2\cdot \mathrm{RuBP}E_1 + s_3\cdot \mathrm{RuBP}E_1\\
\frac{d\mathrm{RuBP}E_1}{dt} &= s_1\cdot \mathrm{RuBP}\cdot E_1 - s_2\cdot \mathrm{RuBP}E_1 - s_3\cdot \mathrm{RuBP}E_1\\
\frac{d\mathrm{PGA}}{dt} &= 2\cdot s_3\cdot \mathrm{RuBP}E_1 - s_4\cdot \mathrm{PGA}\cdot E_2 + s_5\cdot \mathrm{PGA}E_2 - s_{16}\cdot \mathrm{PGA}\cdot E_6 + s_{17}\cdot \mathrm{PGA}E_6\\
\frac{dE_2}{dt} &= -s_4\cdot \mathrm{PGA}\cdot E_2 + s_5\cdot \mathrm{PGA}E_2 + s_6\cdot \mathrm{PGA}E_2\\
\frac{d\mathrm{PGA}E_2}{dt} &= s_4\cdot \mathrm{PGA}\cdot E_2 - s_5\cdot \mathrm{PGA}E_2 - s_6\cdot \mathrm{PGA}E_2\\
\frac{d\mathrm{DPGA}}{dt} &= s_6\cdot \mathrm{PGA}E_2 - s_7\cdot \mathrm{DPGA}\cdot E_3 + s_8\cdot \mathrm{DPGA}E_3\\
\frac{dE_3}{dt} &= -s_7\cdot \mathrm{DPGA}\cdot E_3 + s_8\cdot \mathrm{DPGA}E_3 + s_9\cdot \mathrm{DPGA}E_3\\
\frac{d\mathrm{DPGA}E_3}{dt} &= s_7\cdot \mathrm{DPGA}\cdot E_3 - s_8\cdot \mathrm{DPGA}E_3 - s_9\cdot \mathrm{DPGA}E_3\\
\frac{d\mathrm{GAP}}{dt} &= s_9\cdot \mathrm{DPGA}E_3 - 5\cdot s_{10}\cdot \mathrm{GAP}^5\cdot E_4 + 5\cdot s_{11}\cdot \mathrm{GAP}E_4 - s_{19}\cdot \mathrm{GAP}\cdot E_7 + s_{20}\cdot \mathrm{GAP}E_7\\
\frac{dE_4}{dt} &= -s_{10}\cdot \mathrm{GAP}^5\cdot E_4 + s_{11}\cdot \mathrm{GAP}E_4 + s_{12}\cdot \mathrm{GAP}E_4\\
\frac{d\mathrm{GAP}E_4}{dt} &= s_{10}\cdot \mathrm{GAP}^5\cdot E_4 - s_{11}\cdot \mathrm{GAP}E_4 - s_{12}\cdot \mathrm{GAP}E_4\\
\frac{d\mathrm{Ru5P}}{dt} &= -s_{13}\cdot \mathrm{Ru5P}\cdot E_5 + s_{14}\cdot \mathrm{Ru5P}E_5 + 3\cdot s_{12}\cdot \mathrm{GAP}E_4\\
\frac{dE_5}{dt} &= -s_{13}\cdot \mathrm{Ru5P}\cdot E_5 + s_{14}\cdot \mathrm{Ru5P}E_5 + s_{15}\cdot \mathrm{Ru5P}E_5\\
\frac{d\mathrm{Ru5P}E_5}{dt} &= s_{13}\cdot \mathrm{Ru5P}\cdot E_5 - s_{14}\cdot \mathrm{Ru5P}E_5 - s_{15}\cdot \mathrm{Ru5P}E_5\\
\frac{dE_6}{dt} &= -s_{16}\cdot \mathrm{PGA}\cdot E_6 + s_{17}\cdot \mathrm{PGA}E_6 + s_{18}\cdot \mathrm{PGA}E_6\\
\frac{d\mathrm{PGA}E_6}{dt} &= s_{16}\cdot \mathrm{PGA}\cdot E_6 - s_{17}\cdot \mathrm{PGA}E_6 - s_{18}\cdot \mathrm{PGA}E_6\\
\frac{dE_7}{dt} &= -s_{19}\cdot \mathrm{GAP}\cdot E_7 + s_{20}\cdot \mathrm{GAP}E_7 + s_{21}\cdot \mathrm{GAP}E_7\\
\frac{d\mathrm{GAP}E_7}{dt} &= s_{19}\cdot \mathrm{GAP}\cdot E_7 - s_{20}\cdot \mathrm{GAP}E_7 - s_{21}\cdot \mathrm{GAP}E_7
\end{aligned} \tag{10}$$

Using the parameters shown in Table 2, the system given by Eqs. (10) does have the capability to obtain multiple positive steady states as can be seen by the two steady states presented in Table 3. Furthermore, Fig. 5 shows the corresponding bifurcation diagram for some of the metabolites, using the sum of x_{E_2} and $x_{\mathrm{PGA}E_2}$ as a bifurcation parameter.

Table 3
Two different positive steady states obtained from the system in Eqs. (10) using the parameters shown in Table 2. The first steady state is unstable while the second one is stable.

Variable	Steady state 1 (mM)	Steady state 2 (mM)
x_{RuBP}	2.1738771	7.6340526
x_{E_1}	3.2184725	1.5737360
$x_{\mathrm{RuBP}E_1}$	2.2935102	3.9382467
x_{PGA}	0.7319781	2.2714297
x_{E_2}	1.3155187	0.7209939
$x_{\mathrm{PGA}E_2}$	0.8484346	1.4429594
x_{DPGA}	0.8031938	2.4924215
x_{E_3}	2.0319109	1.1136257
$x_{\mathrm{DPGA}E_3}$	1.3104660	2.2287516
x_{GAP}	0.6439413	1.2921397
x_{E_4}	4.3510314	0.2296564
$x_{\mathrm{GAP}E_4}$	5.7470699	9.8684449
x_{Ru5P}	1.8031031	6.3319974
x_{E_5}	2.6499371	1.2957393
$x_{\mathrm{Ru5P}E_5}$	1.8883671	3.2425640
x_{E_6}	1.4641405	0.9364545
$x_{\mathrm{PGA}E_6}$	0.5358594	1.0635454
x_{E_7}	1.5754002	1.2367929
$x_{\mathrm{GAP}E_7}$	0.5885531	0.9271604

5.3. Michaelis–Menten Kinetics

When irreversible Michaelis–Menten kinetics is imposed on the model of the Calvin cycle, only the approach based on algebraic geometry is applicable, since analysis of multistationarity cannot be performed with any of the tools described in Section 2. Here we consider two cases: (1) the original model from Zhu et al. (2009) and (2) the modified model from Table 1. Contrary to the analysis of Zhu et al. (2009), here we demonstrate that, with the same set of values for the kinetic parameters, two steady states are possible. Moreover, we show qualitatively similar results for the modified model. In addition, we identify the bifurcation parameters and their corresponding regions. Since the concentration of ATP and NADPH are assumed constant (as are the ratios ADP/ATP and NADPH/NADP), there are no conservation relations.

For the first case, although the concentrations of all five Calvin cycle intermediates, RuBP, PGA, DPGA, GAP, and Ru5P, can serve as bifurcation parameters, only four of them yield bifurcations in

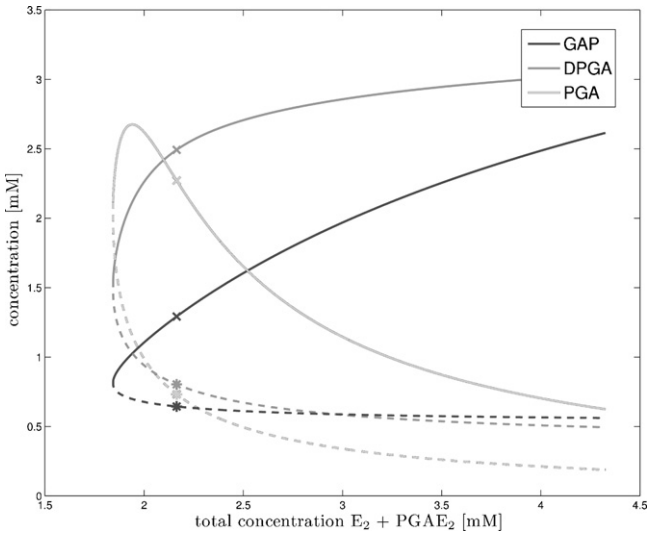

Fig. 5. Bifurcation diagram for system 10 using the parameters from Table 2. Stable steady states are depicted by a solid line, unstable steady states by a dashed line. The stars and crosses mark the concentrations at steady state 1 and 2, respectively (see Table 3). The sum of concentrations of E_2 and $\mathrm{PGA}E_2$ is chosen as a bifurcation parameter.

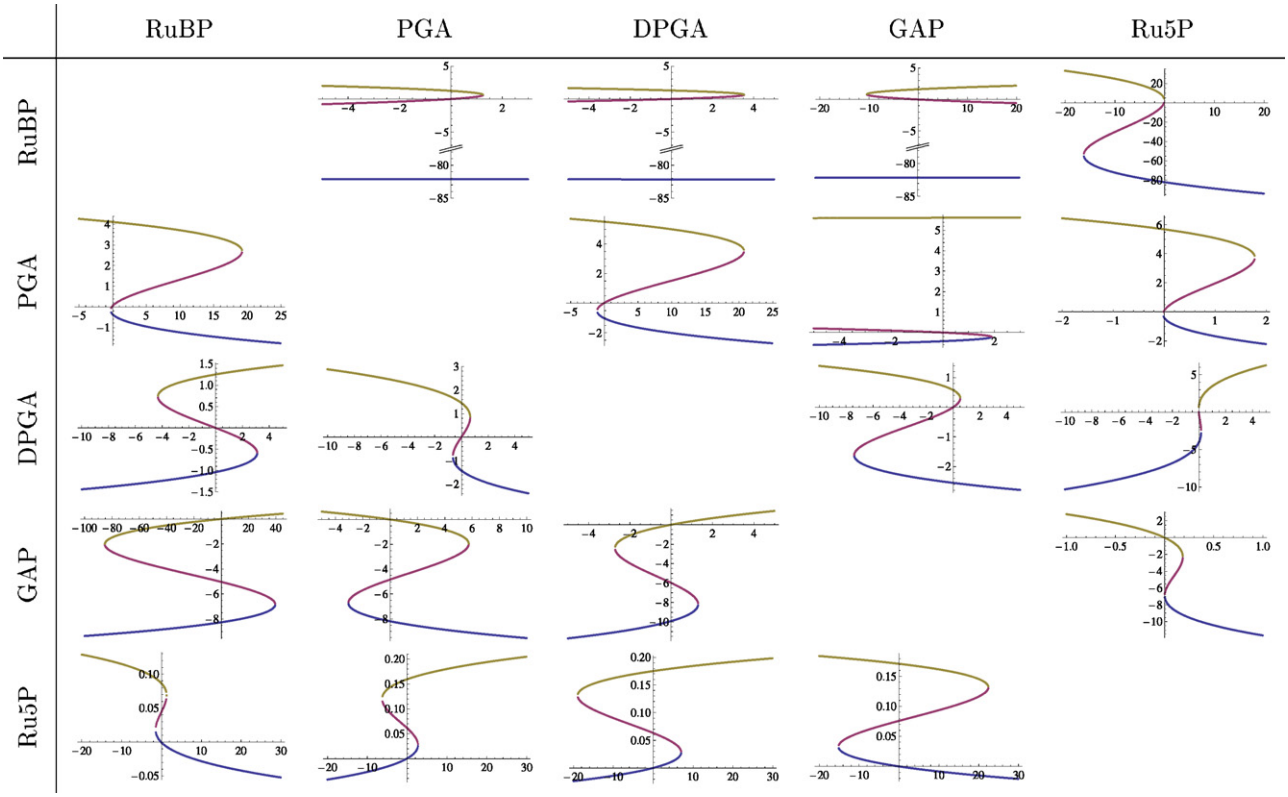

Fig. 6. Bifurcation parameters for the original Calvin cycle model from Zhu et al. (2009) with irreversible Michaelis–Menten kinetics. Since CRNT tools cannot be applied in this case, the curves are obtained by solving the system of Gröbner bases. In each of the subfigures, the steady state concentrations of two metabolites are plotted against each other using the parameters from Zhu et al. (2009). Multistationarity is confirmed by detecting three steady states (yellow, red, and blue line). For instance, for positive values of x_{Ru5P}, there are at least two positive steady states for the remaining four metabolites. The stability of these steady states cannot be determined by our approach alone.

positive ranges for the concentration of the remaining metabolites. Clearly, there are twenty possible bifurcation diagrams due to the pairwise combinations of the five Calvin cycle intermediates, as shown by the individual plots inlaid in Fig. 6. By means of an algebraic transformation, detailed below, the dependencies to the other intermediates can be eliminated. Eleven of these twenty combinations show multistationarity for positive concentration values. This conclusion holds when one considers the definition of physiologically plausible concentrations given in Zhu et al. (2009), taking the range (0.0001–5) mM for all metabolites (this range gives the lower and upper bounds of the solution found *therein*).

However, for physiologically plausible concentrations, $x_{RuBP} \in [0.6, 6.0]$, $x_{PGA} \in [1.4, 12.0]$, $x_{DPGA} \in [0.8, 1.4]$, $x_{GAP} \in [0.032, 0.04]$, and $x_{Ru5P} \in [0.01, 0.2]$ mM as given in Zhu et al. (2007), there exist eight cases—*e.g.*, x_{PGA} given in terms of the bifurcation parameter x_{RuBP}—where the concentrations of the two depicted metabolites fall in the respective physiological ranges. Note that, as seen in the last row of Fig. 6, for physiologically plausible values of x_{Ru5P}, there are at least two physiologically plausible steady states for the remaining four metabolites.

We point out that in seven out of the twenty cases, there exists no steady state in the intersection of the physiological ranges for the pair of considered metabolites. In addition, the combinations for which a single steady state exists for the physiologically plausible range include the following five: x_{RuBP} as a function of the bifurcation parameter x_{GAP}, x_{PGA} in terms of x_{GAP}, x_{DPGA} depending on x_{RuBP} and x_{Ru5P}, respectively, and x_{GAP} with respect to x_{RuBP}.

Like in the first case, for the modified model all five Calvin cycle intermediates can serve as bifurcation parameters. Only four of them yield bifurcations in positive ranges for the concentration of the remaining metabolites GAP has at most one positive steady state. There are again twenty possible bifurcation diagrams due to the pairwise combinations of the five Calvin cycle intermediates with no further dependencies, as shown by the individual plots inlaid in Fig. 7. Nine of these twenty combinations show multistationarity for positive concentration values. For the physiologically plausible concentrations, there exists only one case—x_{Ru5P} given in terms of the bifurcation parameter x_{PGA}—where the concentrations of the two depicted metabolites fall in the respective physiological ranges.

We point out that in eleven out of the twenty cases, there exists no steady state in the intersection of the physiological ranges for the pair of considered metabolites. Hence, there are obviously eight combinations for which a single steady state exists for the physiologically plausible range.

To obtain these results, we calculated the Gröbner bases, V, for differently ordered monomials (*i.e.*, the concentrations for the Calvin cycle intermediates), as described in Algorithm 1. For the Michaelis–Menten kinetics, each basis is given by a set of polynomials p and rational functions r. These polynomials and rational functions include the last monomial of the order and the concentration for one Calvin cycle intermediates—the bifurcation parameter. Thus, each pairwise combination of two intermediate concentrations occurs and the Gröbner basis contains at least one polynomial in terms of the fixed intermediate, last monomial of the order, and the bifurcation parameter.

To investigate the multistationarity of the original model from Zhu et al. (2009) for the combination of x_{PGA} as function of bifurcation parameter x_{RuBP} in the physiologically plausible concentration ranges, we use the Gröbner basis for the monomial order (Ru5P,*DPGA*,RuBP,GAP,PGA). The used polynomial basis element for this dependent combination of intermediates is the seventh

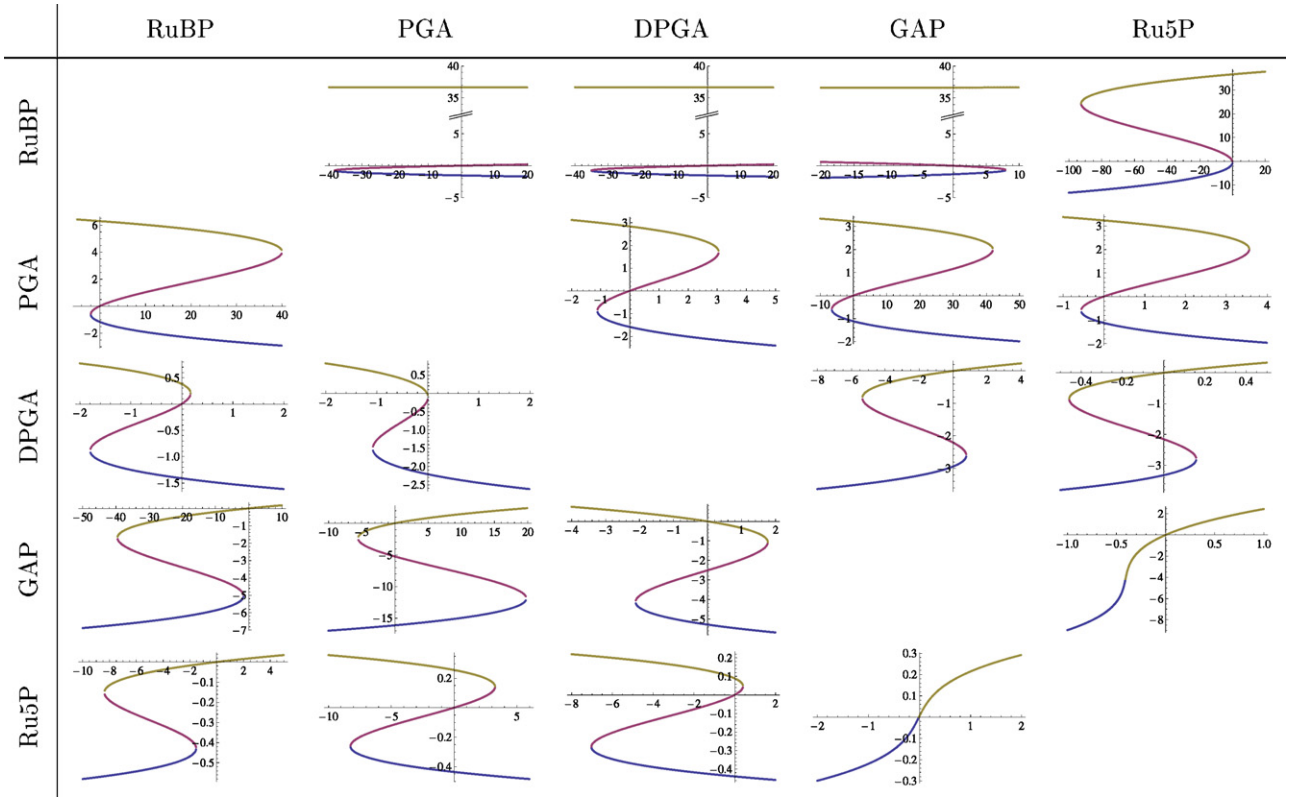

Fig. 7. Bifurcation parameters for the modified Calvin cycle model as described in Table 1 with irreversible Michaelis–Menten kinetics. In each of the subfigures, the steady state concentrations of two metabolites are plotted against each other, like in (Fig. 6), using the parameters from Zhu et al. (2009). Multistationarity is confirmed by detecting three steady states (yellow, red, and blue line). For instance, for positive values of x_{PGA}, there are at least two positive steady states for the remaining four metabolites.

element, given by

$$p = -2.2079 \cdot x_{PGA} - 6.33023 \cdot {x_{PGA}}^2 + 1.66547 \cdot {x_{PGA}}^3 + 1.0 \cdot x_{RuBP}. \quad (11)$$

We set the polynomial in Eq. (11) to zero and solve it for $x_{PGA} = f(x_{RuBP})$. The three arising solutions were then plotted as a function of x_{RuBP} and were evaluated on the physiologically plausible intervals for RuBP and *PGA* concentrations (shown in Fig. 6 row: PGA, column: RuBP). These calculations were performed with Mathematica 7.0. A detailed summary of computations is provided as a Supplementary file. The notebook to reproduce the bifurcation diagrams is available upon request (Table 4).

Following this approach, the results presented in Figs. 6 and 7 serve as a rigorous proof of the capacity for multistationarity in this model of the Calvin cycle. Moreover, these findings demonstrate the reason why previous studies failed to determine the regions of bifurcation by "trial-and-error" approaches. While solving systems of polynomials, as in Zhu et al. (2009), may yield partial results, any finding which employs Gröbner bases is exhaustive due to the representational power of this mathematical construct.

5.4. Mass Action with Diffusion

Spatiotemporal dynamics of the Calvin cycle can be investigated in two principle ways: The first consists of considering a model augmented with different cellular compartments, yielding a partition of the metabolic pools. The second, which we pursue in this section, includes the study of metabolite diffusion.

Metabolite diffusion results in a fundamentally different view of multistationarity compared to that of Sections 5.1–5.3. We determine the existence of symmetry breaking instabilities in the investigated metabolic network, *i.e.*, instabilities due to diffusion. Characteristic examples of such instabilities for biochemical reactions include: a substrate and product-inhibited enzyme reaction and the product-activated enzyme reaction catalyzed by phosphofructokinase in the glycolytic cycle (Prigogine et al., 1969). The basic theoretical question is in fact, whether the steady-state concentrations may, with increasing values of chemical constraints (given affinities or free-energies of the over-all reactions), still be obtained by a gradual modification of the law of mass action. Symmetry breaking instabilities have been investigated for chemical (Bar-Eli, 1985; Dolnik and Marek, 1988; Crowley and Epstein, 1989; Maini and Chau, 1997), gene-regulatory(Koseska et al., 2007), and metabolic networks (Tsaneva-Atanasova et al., 2006). They have also been observed in biological processes in which slow diffusion is present (Shiferaw and Karma, 2006; Kondo and Asi, 1995).

Unlike the case of homogeneous perturbations, when the system moves from one to another homogeneous steady state, for inhomogeneous perturbations the system goes from a homogeneous to an inhomogeneous steady state (IHSS). The instabilities are a result of the symmetry breaking of the steady state in the system through a pitchfork bifurcation. Thus, the unstable homogeneous steady state splits into two additional branches, which then gain stability via Hopf bifurcations. If the complete bifurcation structure of the system cannot be obtained due to computational or experimental restrictions, the existence of the inhomogeneous steady state could be easily misinterpreted as two separate steady states. Here, we define conditions under which the Calvin cycle can be characterized with the occurrence of an IHSS.

In plants, the chloroplast thylakoid membrane is the site of light-dependent photosynthetic reactions coupled to ATP synthesis. Recent experimental studies have confirmed that (i) the chloroplast thylakoid ATP/ADP carrier supplies the thylakoid lumen with stromal ATP in exchange for ADP and (ii) increased concen-

Table 4
Number of multiple, single and no steady state(s) as depicted in Figs. 6 and 7. The respective entries are obtained by evaluating two different domains—positive concentrations and physiologically plausible concentrations of the intermediates.

Model variants	Ranges	Multiple (steady states)	Single (steady states)	No (steady states)
Zhu et al. (2009)	Positive	11	6	3
	Physiologically plausible	8	5	7
Table 1	Positive	9	9	2
	Physiologically plausible	1	8	11

trations of ATP in the stroma cause activation of RuBisCo activase (Thuswaldner et al., 2007; Yin et al., 2010). Since ATP, as the principle energy compound, diffuses between cellular compartments (Basshama et al., 1968) and is essential for the light-independent photosynthetic reactions, we analyzed the effects of ATP diffusion on the existence of inhomogeneous steady states. We extend the model presented in Fig. 1 by the following reaction:

$$\mathrm{ADP} \xrightarrow{k_8} \mathrm{ATP}. \tag{12}$$

Furthermore, the two kinases are not simplified and now read as in the second column of Table 1.

By assuming a Fick type of diffusion law, the equations describing the balance between reaction rates and diffusion can be written as follows:

$$\begin{aligned}
\frac{\partial x_{\mathrm{RuBP}}}{\partial t} &= -k_1 \cdot x_{\mathrm{RuBP}} + k_5 \cdot x_{\mathrm{Ru5P}} \cdot x_{\mathrm{ATP}} \\
\frac{\partial x_{\mathrm{PGA}}}{\partial t} &= 2 \cdot k_1 \cdot x_{\mathrm{RuBP}} - k_2 \cdot x_{\mathrm{PGA}} \cdot x_{\mathrm{ATP}} - k_6 \cdot x_{\mathrm{PGA}} \\
\frac{\partial x_{\mathrm{DPGA}}}{\partial t} &= -k_3 \cdot x_{\mathrm{DPGA}} + k_2 \cdot x_{\mathrm{PGA}} \cdot x_{\mathrm{ATP}} \\
\frac{\partial x_{\mathrm{GAP}}}{\partial t} &= k_3 \cdot x_{\mathrm{DPGA}} - k_7 \cdot x_{\mathrm{GAP}} - 5 \cdot k_4 \cdot x_{\mathrm{GAP}}^5 \\
\frac{\partial x_{\mathrm{Ru5P}}}{\partial t} &= 3 \cdot k_4 \cdot x_{\mathrm{GAP}}^5 - k_5 \cdot x_{\mathrm{Ru5P}} \cdot x_{\mathrm{ATP}} \\
\frac{\partial x_{\mathrm{ATP}}}{\partial t} &= -k_2 \cdot x_{\mathrm{PGA}} \cdot x_{\mathrm{ATP}} - k_5 \cdot x_{\mathrm{Ru5P}} \cdot x_{\mathrm{ATP}} + k_8 (c - x_{\mathrm{ATP}}) + D_{\mathrm{ATP}} \cdot \left(\frac{\partial^2 x_{\mathrm{ATP}}}{\partial R^2} \right)
\end{aligned} \tag{13}$$

In the system given by Eqs. (13), D_{ATP} is the diffusion coefficient of ATP, assumed to be constant, such that ADP = c − ATP, where c is the constant amount of adenosine nucleotides. Here, R indicates the diffusion coordinate. For this system of polynomials, we find the following parameterization at steady state:

$$\begin{aligned}
x_{\mathrm{PGA}} &= \frac{k_8 \left(5 \cdot k_1 x_{\mathrm{RuBP}} + 3 \cdot k_7 \cdot \sqrt[5]{\frac{k_1 x_{\mathrm{RuBP}}}{3 \cdot k_4}}\right)}{k_2 \left(3 \cdot c \cdot k_8 - 8 \cdot k_1 \cdot x_{\mathrm{RuBP}} - 3 \cdot k_7 \cdot \sqrt[5]{\frac{k_1 x_{\mathrm{RuBP}}}{3 \cdot k_4}}\right)} \\
x_{\mathrm{DPGA}} &= \frac{5 \cdot k_1 \cdot x_{\mathrm{RuBP}} \cdot \sqrt[5]{3 \cdot k_4} + 3 \cdot k_7 \cdot \sqrt[5]{k_1 x_{\mathrm{RuBP}}}}{3 \cdot k_3 \cdot \sqrt[5]{3 \cdot k_4}} \\
x_{\mathrm{GAP}} &= \sqrt[5]{\frac{k_1 \cdot x_{\mathrm{RuBP}}}{3 \cdot k_4}} \\
x_{\mathrm{Ru5P}} &= \frac{3 \cdot k_1 \cdot k_8 \cdot \mathrm{RuBP}}{k_5 \left(3 \cdot c \cdot k_8 - 8 \cdot k_1 \cdot x_{\mathrm{RuBP}} - 3 \cdot k_7 \cdot \sqrt[5]{\frac{k_1 \cdot x_{\mathrm{RuBP}}}{3 \cdot k_4}}\right)} \\
x_{\mathrm{ATP}} &= c - \frac{8 \cdot k_1 x_{\mathrm{RuBP}}}{3 \cdot k_8} - \frac{k_7}{k_8} \cdot \sqrt[5]{\frac{k_1 \cdot x_{\mathrm{RuBP}}}{3 \cdot k_4}},
\end{aligned} \tag{14}$$

and a quintic equation for x_{RuBP} of the form $Az^5 + Bz + C = 0$, where $z = \sqrt[5]{x_{\mathrm{RuBP}}}$. One may show that this equation has only one positive solution for x_{RuBP}, which facilitates the computation of the time-independent homogeneous solution given in Table 5.

We now consider the linear stability of this steady uniform solution with respect to space and time-dependent perturbations. Therefore, it is sufficient to consider perturbations of the form:

$$x = x_{eq} + X \exp[\omega \cdot t + i(r/\lambda)], \tag{15}$$

where x corresponds to the concentration of any variable in the system given by Eqs. (13), and x_{eq} denotes the steady state concentrations, provided we consider affinities small with respect to kT. Let X be the perturbation amplitude which is assumed to satisfy $|X/x_{eq}| \ll 1$, and ω and λ are the perturbation frequency and wavelength correspondingly. If an instability occurs, the perturbed system will, at some moment, be in a state of marginal stability, corresponding to $\omega = 0$. Hence, the secular (characteristic) equations for the system in Eqs. (13), obtained by the perturbation of each concentration according to Eq. (15) and linearized with respect to X in the marginal state, provides the following relation:

$$k_6 = \frac{(k_8 + (D_{\mathrm{ATP}}/\lambda^2)) \cdot (k_7 - 5 \cdot k_4 \cdot x_{\mathrm{GAP}_{eq}}^4)}{3 \cdot (30 \cdot k_4 \cdot x_{\mathrm{GAP}_{eq}}^4 + k_7)}, \tag{16}$$

for the rate constants, diffusion coefficient, and the wavelength λ.

Note that the relation described in Eq. (16) holds only in the marginal state, and separates a root $\omega < 0$ from a root $\omega > 0$. Thus, for a given set of parameters, the critical value of the wavelength λ at which the instability begins can be estimated from:

$$\lambda_c^2 = \frac{(k_7 - 5 \cdot k_4 \cdot x_{\mathrm{GAP}_{eq}}^4) \cdot D_{\mathrm{ATP}}}{3 \cdot k_6 \cdot (30 \cdot k_4 \cdot x_{\mathrm{GAP}_{eq}}^4 + k_7) - k_8 \cdot k_7 + 5 \cdot k_4 \cdot k_8 \cdot x_{\mathrm{GAP}_{eq}}^4}. \tag{17}$$

From Eq. (17), one can conclude that the critical wavelength, λ_c, depends on both the kinetic parameters and the diffusion coefficient. As a result, the ratio between the diffusion coefficient and the reaction rates determines the wavelengths at which the instability occurs in the system.

6. Discussion

The results obtained from applying our general method to a model of the Calvin cycle, endowed with a hierarchy of kinetics, are summarized in Table 6. The presented findings are corollaries of well-established theorems relating the underlying structure of the network with its dynamical features. For the model with mass action kinetics, we not only established that a single steady state exists, but also determined the conditions for its stability. Interestingly, weakening the mass-action assumption by explicitly

Table 5
Steady state solution derived from Eqs. (13).

Variable	Steady state (mM)
x_{RuBP}	0.01982
x_{PGA}	0.03313
x_{DPGA}	0.03236
x_{GAP}	0.38252
x_{Ru5P}	0.02235
x_{ATP}	0.41904

Table 6
Summary of results regarding multistationarity for a model of the Calvin cycle with a hierarchy of kinetic laws. The first column gives the hierarchy of kinetics, from simplest to more involved: mass action (MA), Michaelis–Menten via mass action (MM-MA), Michaelis–Menten (MM), and mass action with diffusion (MAd). The considered type of instabilities and the existence of multistationarity are given in the second and third column, respectively. The methods used to establish the potential for multistationarity and the bifurcation parameters/regions are listed in the last column. Provable results are obtained for all kinetics considered in the hierarchy.

Kinetics	Instability	Multistationarity	Support
MA	Homogeneous	NO	CRNT and algebraic geometry
MM-MA	Homogeneous	YES	CRNT and stoichiometric generators
MM	Homogeneous	YES	algebraic geometry
MAd	Inhomogeneous	YES	algebraic geometry

modeling enzyme mechanisms leads to multiple positive steady states. This is a result of applying the subnetwork analysis in conjunction with CRNT. By employing methods from algebraic geometry, we also demonstrated the existence of multistationarity in the model with Michaelis–Menten kinetics and identified the bifurcation parameters together with the physiologically plausible regions of the parameter space which supports more than one steady state. As indicated in Section 4, our approach warrants application of other methods to resolve the stability of the determined steady states. Therefore, our findings only partially settle the issue of multistability of the Calvin cycle, since we only consider one model and derive the conditions for its ability to support multistationarity.

Besides the simplicity of the considered model and the coarse modeling of the Michaelis–Menten kinetics, one further concern arises from the parameter values and the steady state concentrations of the metabolites. Since CRNT only aims at answering whether or not multiple positive steady states can occur, the resulting values for the parameters and metabolite concentrations may lie outside of any physiologically meaningful range. Nevertheless, there is some freedom in choosing those parameters, *e.g.*, for reactions not included in the subnetwork induced by an elementary flux mode. This can be further exploited to test whether multistationarity also occurs for physiologically feasible parameter values and metabolite concentrations.

We note that an isolated reaction network of the form of $A+E \leftrightarrows AE \rightarrow B$, which is exactly the set of reactions that were included to emulate Michaelis–Menten kinetics, does not support multiple steady states on its own (Craciun et al., 2006). Therefore, the fact that multiple steady states exist for the model with Michaelis–Menten via mass action kinetics and not with mass action kinetics implies that multistationarity, for the former kinetic law, does not arise from local structural properties but rather from the overall structure of the entire network.

Our approach allows for a tractable analytical analysis of models with Michaelis–Menten kinetics. In this way, we were able to identify the physiologically plausible regions of the parameter space in which bifurcation could occur. The obtained results with respect to the bifurcation parameters, shown in Fig. 6, can help the design of validation experiments for multistationarity in plant cells. For instance, a validation experiment with isolated chloroplasts and concentration changes of the bifurcation parameter *PGA*, for which there exists a chloroplast transporter, can now be readily undertaken.

For the reaction diffusion model, we established theoretical results determining the ratio between the diffusion coefficient of ATP and the reaction rates which, in turn, determines the wavelengths at which inhomogeneous instability could occur. Eliciting biological conclusions from these results would be premature, as we only consider diffusion systems in one dimension. The problem of developing a model to account for more realistic types of diffusion, not only of ATP but also other Calvin cycle intermediates, remains to be addressed with methods similar to those presented here.

Rigorous analysis of multistationarity on metabolic networks allows for altering the final outcome of metabolic processes. Therefore, multistationarity presents a dynamic feature amenable to biotechnological application, specifically increased biomass production. However, as pointed in our analysis, any conclusions regarding multistationarity are tightly coupled with the details of the employed model, and warrant caution in design of experimental metabolic engineering procedures.

Finally, although we studied a model of the Calvin cycle in which a hierarchy of kinetics is embedded, our approach is not limited to metabolic networks. In principle, the pressing question of multistationarity can be analyzed with such an approach for any biological network modeled with mass action or Michaelis–Menten kinetics.

Acknowledgements

AA, AK, JK, JS and ZN and are supported by the *Go* FORSYS project funded by the Federal Ministry of Education and Research, Grant no. 0313924. SG and JS are supported by the ColoNET project funded by the Federal Ministry of Education and Research, Grant no. 0315417F. ZN acknowledges financial support from the Max Planck Society.

Appendix A. Supplementary data

Supplementary data associated with this article can be found, in the online version, at doi:10.1016/j.biosystems.2010.10.015.

References

Acuña, V., Chierichetti, F., Lacroix, V., Marchetti-Spaccamela, A., Sagot, M.-F., Stougie, L., 2008. Modes and cuts in metabolic networks: complexity and algorithms. Biosystems (August). URL http://dx.doi.org/10.1016/j.biosystems.2008.06.015.

Bagowski, C.P., Besser, J., Frey, C.R., Ferrell, J.E., 2003. The JNK cascade as a biochemical switch in mammalian cells ultrasensitive and all-or-none responses. Curr. Opin. Biol. 13, 315–320.

Bagowski, C.P., Ferrell, J.E., James, E., 2001. Bistability in the JNK cascade. Curr. Opin. Biol. 11, 1176–1182.

Bar-Eli, K., 1985. On the stability of coupled chemical oscillators. Physica D 14, 242–252.

Basshama, J., Kirka, M., Jensen, R., 1968. Photosynthesis by isolated chloroplasts I. Diffusion of labeled photosynthetic intermediates between isolated chloroplasts and suspending medium. Biochem. Biophys. Acta (BBA)-Bioenerg. 153, 211–218.

Berg, J., Tymoczko, J., Stryer, L., 2002. Biochemistry, 5th edition. W.H. Freeman and Company, New York.

Chatterjee, A., Kaznessis, Y.N., Hu, W.-S., 2008. Tweaking biological switches through a better understanding of bistability behavior. Curr. Opin. Biotechnol. 19, 475–481.

Conradi, C., Flockerzi, D., Raisch, J., Stelling, J., 2007. Subnetwork analysis reveals dynamic features of complex (bio)chemical networks. Proc. Natl. Acad. Sci. U.S.A. 104 (December (49)), 19175–19180. URL http://dx.doi.org/10.1073/pnas.0705731104.

Cox, D., Little, J., O'Shea, D., 1991. Ideals, Varieties and Algorithms: An Introduction to Computational Algebraic Geometry and Commutative Algebra. Springer-Verlag, New York, USA.

Craciun, G., Tang, Y., Feinberg, M., 2006. Understanding bistability in complex enzyme-driven reaction networks. Proc. Natl. Acad. Sci. U.S.A. 103 (June (23)), 8697–8702. URL http://dx.doi.org/10.1073/pnas.0602767103.

Crowley, M.F., Epstein, I., 1989. Experimental and theoretical studies of a coupled chemical oscillator: phase death, multistability, and in-phase and out-of-phase entrainment. J. Phys. Chem. 93, 2496–2502.

Dolnik, M., Marek, M., 1988. Extinction of oscillations in forced and coupled reaction cells. J. Phys. Chem. 92, 2452–2455.

Feinberg, M., 1995a. The existence and uniqueness of steady states for a class of chemical reaction networks. Arch. Ration. Mech. Anal. 132, 311–370.

Feinberg, M., 1995b. Multiple steady states for chemical reaction networks of deficiency one. Arch. Ration. Mech. Anal. 132, 371–406.

Feinberg, M., Ellison, P., 2000. The chemical reaction network toolbox (CRNT). http://www.che.eng.ohio-state.edu/feinberg/crnt/ version 1.1.

Flügge, U.I., Freisl, M., Heldt, H.W., 1980. Balance between metabolite accumulation and transport in relation to photosynthesis by isolated spinach chloroplasts. Plant Physiol. 65 (April 4), 574–577.
Gatermann, K., Wolfrum, M., 2005. Bernstein's second theorem and Viro's method for sparse polynomial systems in chemistry. Adv. Appl. Math. 34, 252–294.
Grimbs, S., Selbig, J., Bulik, S., Holzhütter, H.-G., Steuer, R., 2007. The stability and robustness of metabolic states: identifying stabilizing sites in metabolic networks. Mol. Syst. Biol. 3, 146. URL http://dx.doi.org/10.1038/msb4100186.
Heinrich, R., Schuster, S., 1996. The Regulation of Cellular Systems. Chapman and Hall, New York, USA.
Heldt, H.W., Chon, C.J., Maronde, D., 1977. Role of orthophosphate and other factors in the regulation of starch formation in leaves and isolated chloroplasts. Plant Physiol. 59 (June 6), 1146–1155.
Horn, F., Jackson, R., 1972. General mass action kinetics. Arch. Ration. Mech. Anal. B47, 81–116.
Kaneko, K., Yomo, T., 1994. Cell division, differentiation and dynamic clustering. Physica D 75, 89–102.
Klamt, S., Stelling, J., 2002. Combinatorial complexity of pathway analysis in metabolic networks. Mol. Biol. Rep. 29 (1–2), 233–236.
Kondo, S., Asi, R., 1995. A vialbe reaction-diffusion wave on the skin of pomacanthus, the marine angelfish. Nature 376, 767–768.
Koseska, A., Ullner, E., Volkov, E., Kurths, J., Garcia-Ojalvo, J., 2010. Cooperative differentiation through clustering in multicellular populations. J. Theor. Biol. 263, 189–202.
Koseska, A., Volkov, E., Zaikin, A., Kurths, J., 2007. Inherent multistability in arrays of autoinducer coupled genetic oscillators. Phys. Rev. E 75, 031916.
Li, H.Y., Ho, P.Y., 2000. Subnetwork analysis for the determination of multiple steady states in complex reaction networks. Ind. Eng. Chem. Res. 39, 3291–3297.
Maini, P.K., P, K.J., Chau, H.N.P., 1997. Spatial pattern formation in chemical and biological systems. J. Chem. Soc., Faraday Trans. 93 (20), 3601–3610.
Martinez-Forero, I., Pelaez-Lopez, A., Villoslada, P., 2010. Steady state detection of chemical reaction networks using simplified analytical method. PLoS ONE 5, e10823.
Nakajima, A., Kaneko, K., 2008. Regulative differentiation as bifurcation of interacting cell population. J. Theor. Biol. 253, 779–787.
Olçer, H., Lloyd, J.C., Raines, C.A., 2001. Photosynthetic capacity is differentially affected by reductions in sedoheptulose-1,7-bisphosphatase activity during leaf development in transgenic tobacco plants. Plant Physiol. 125 (February 2), 982–989.
Palsson, B.O., 2000. The challenges of in silico biology. Nat. Biotechnol. 18, 1147–1150.
Pettersson, G., Ryde-Pettersson, U., 1988. A mathematical model of the Calvin photosynthesis cycle. Eur. J. Biochem. 175 (August 3), 661–672.
Poolman, M.G., Fell, D.A., Thomas, S., 2000. Modelling photosynthesis and its control. J. Exp. Bot. 51 Spec No (February), 319–328.
Poolman, M.G., Olçer, H., Lloyd, J.C., Raines, C.A., Fell, D.A., 2001. Computer modelling and experimental evidence for two steady states in the photosynthetic Calvin cycle. Eur. J. Biochem. 268 (May 10), 2810–2816.
Prigogine, I., Lefever, R., Goldbeter, A., Herschkowitz-Kaufman, M., 1969. Symmetry breaking instabilities in biological systems. Nature 223, 913–916.
Prigogine, I., Nicolis, G., 1967. On symmetry breaking instabilities in dissipative systems. J. Chem. Phys. 46, 3542–3550.
Schuster, S., Fell, D.A., Dandekar, T., 2000. A general definition of metabolic pathways useful for systematic organization and analysis of complex metabolic networks. Nat. Biotechnol. 18, 326–332.
Shiferaw, Y., Karma, A., 2006. Turing instabilities mediated by voltage and calcium diffusion in paced cardiac cells. PNAS 103 (15), 5670–5675.
Soranzo, N., Altafini, C., 2009. ERNEST: a toolbox for chemical reaction network theory. Bioinformatics, btp513v1.
Stitt, M., Krapp, A., 1999. The interaction between elevated carbon dioxide and nitrogen nutrition: the physiological and molecular background. Plant Cell Environ. 22, 465–487.
Thomson, M., Gunawardena, J., 2009. Unlimited muultistability in multisite phosphorylation systems. Nature 460, 274–277.
Thuswaldner, S., Lagerstedt, J.O., Rojas-Stütz, M., Leborgne-Castel, K.B.C.D.N., Mishra, A., Marty, F., Schoefs, B., Adamska, I., Persson, B.L., Spetea, C., 2007. Identification, expression, and functional analyses of a thylakoid atp/adp carrier from arabidopsis. J. Biol. Chem. 282, 8848–8859.
Tsaneva-Atanasova, K., Zimliki, A.L., Bertram, R., Sherman, A., 2006. Diffusion of calcium and metabolites in pancreatic islets: killing oscillations with a pitchfork. Biophys. J. 90, 3434–3446.
Tyson, J.J., Chen, K.C., Novak, B., 2003. Sniffers, buzzers, toggles and blinkers: dynamics of regulatory and signaling pathways in the cell. Curr. Opin. Cell Biol. 15, 221–231.
van Kamp, A., Schuster, S., 2006. Metatool 5.0: fast and flexible elementary modes analysis. Bioinformatics 22, 1030–1931.
Yin, L., Lundin, B., Bertrand, M., Nurmi, M., Solymosi, K., Kangasjarvi, S., Aro, E.-M., Schoefs, B., Spetea, C., 2010. Role of thylakoid atp/adp carrier in photoinhibition and photoprotection of photosystem ii in arabidopsis. Plant Phys. 153 (2), 666.
Zhu, X.-G., Alba, R., de Sturler, E., 2009. A simple model of the CAlvin cycle has only one physiologically feasible steady state under the same external conditions. Nonl. Anal. RWA 10 (3), 1490–1499.
Zhu, X.-G., de Sturler, E., Long, S.P., 2007. Optimizing the distribution of resources between enzymes of carbon metabolism can dramatically increase photosynthetic rate: a numerical simulation using an evolutionary algorithm. Plant Physiol. 145 (October (2)), 513–526. URL http://dx.doi.org/10.1104/pp.107.103713.